# CrystEngComm

Supporting Information for

Control of morphology, specific surface area and agglomeration of precipitated calcium carbonate crystals through a multiphase carbonation process

Meisam Ghiasi, Mahmoud Abdollahy [*], Mohammad Reza Khalesi, Ehsan Ghiasi

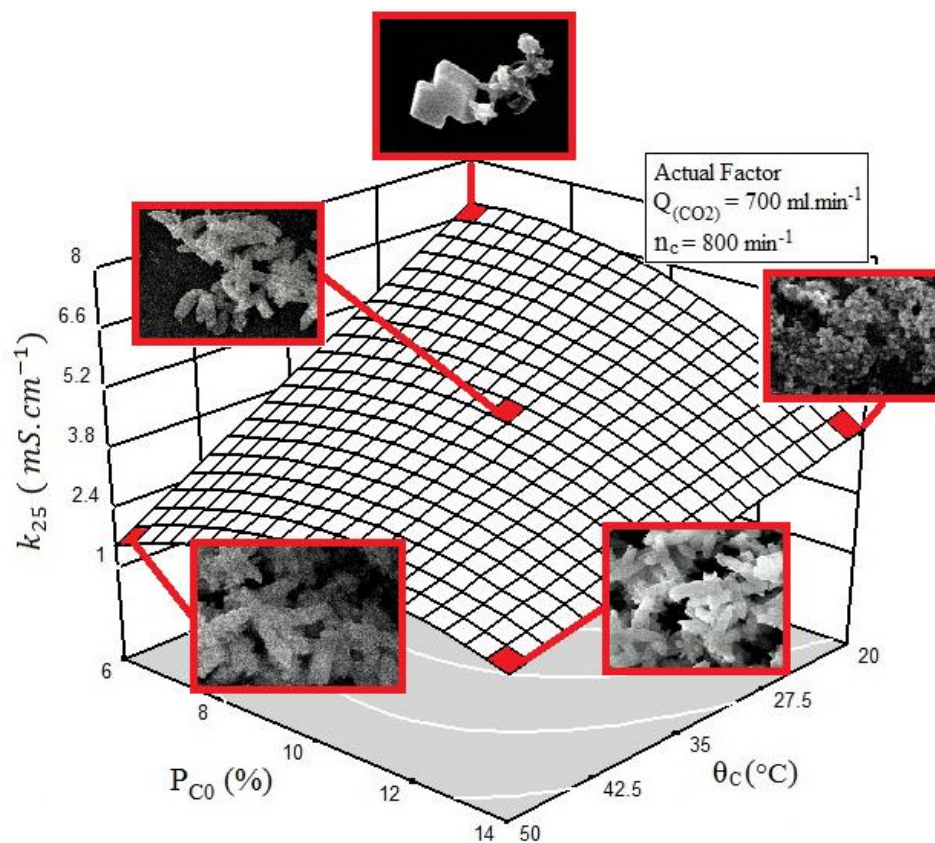Department of Mining Engineering, Tarbiat Modares University, Tehran, Iran

Supporting information S1:
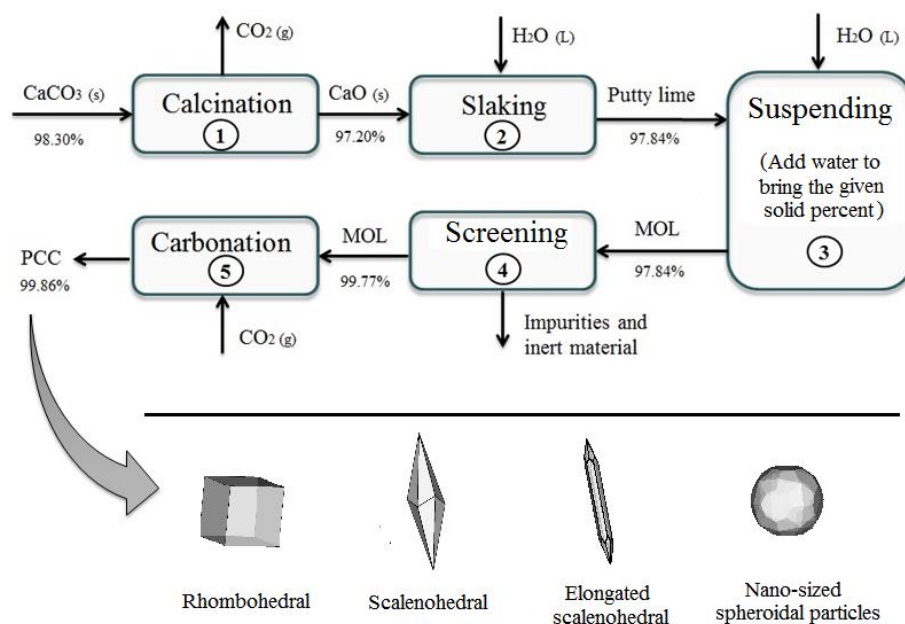
Figure S1. Schematic of PCC production from limestone (The purity of the produced materials is shown in each step)
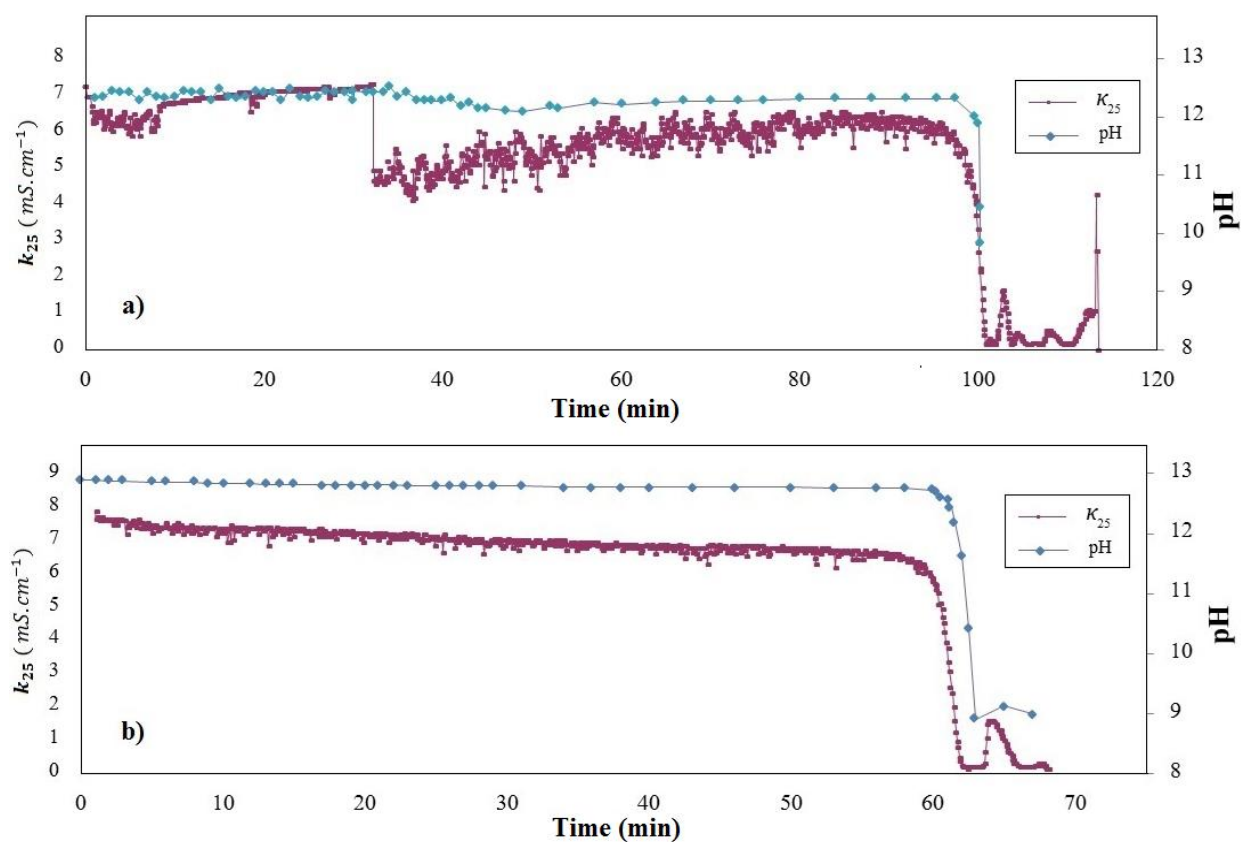
[*] Corresponding author. Tel.: +98 9122 4995 88; fax: +98 21 82 88 43 24

E-mail address: MINMABD@modares.ac.ir (M. Abdollahy).

Supporting information S2:

Figure S2. conductivity as a function of temperature (θ_C) and initial solid percent of the MOL suspension (P_{C0}) with SEM micrographs of the resulting PCC crystals.
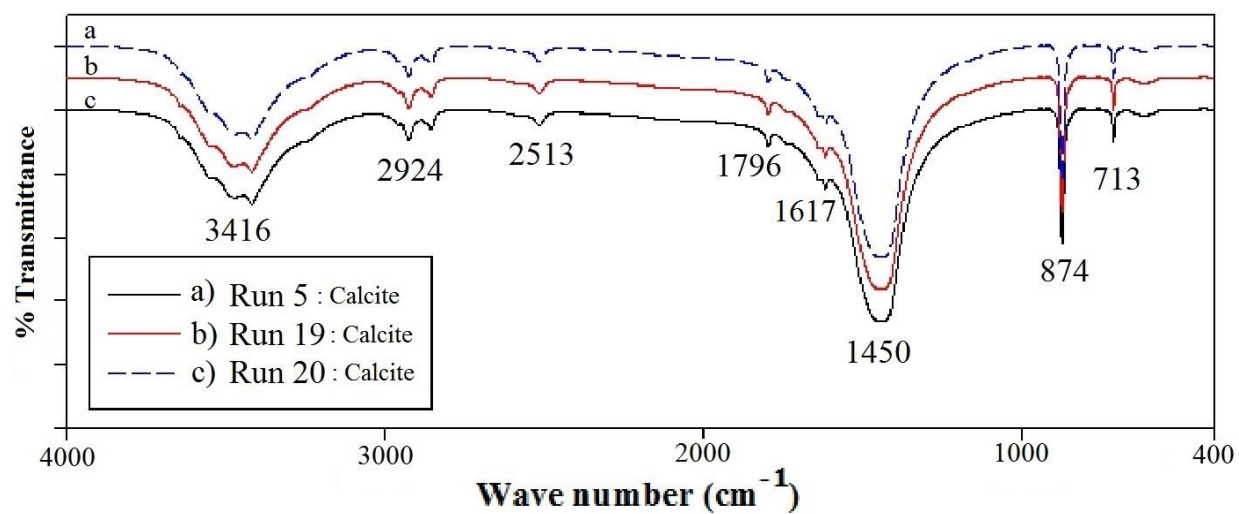
Supporting information S3:

Figure S3. pH and conductivity variations during PCC synthesis at 20°C. a) Conductivity drastically changed during reaction time. b) Steady state conductivity production and supersaturation mode by eliminating all shocks to the precipitation system.
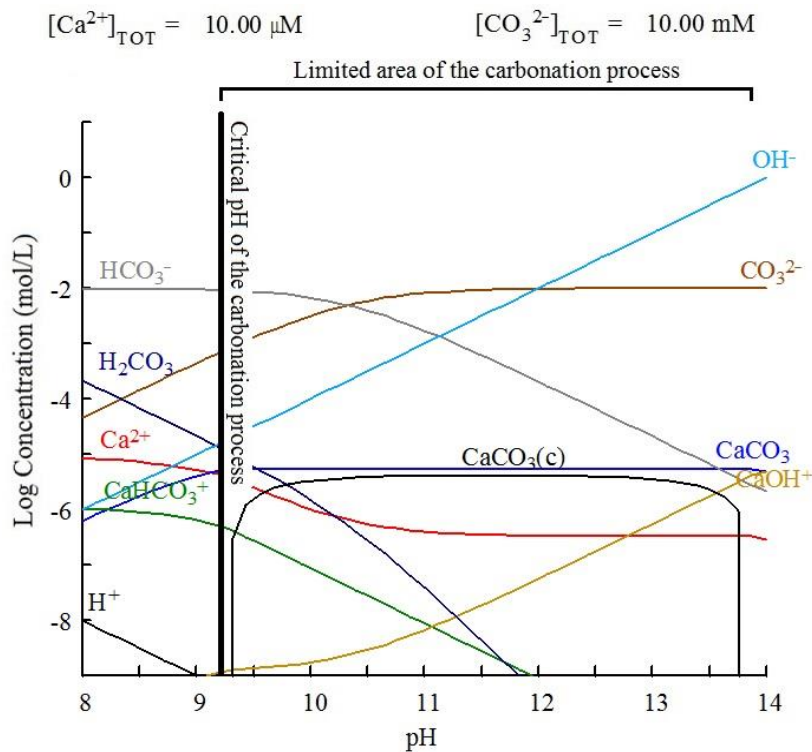
Supporting information S4:
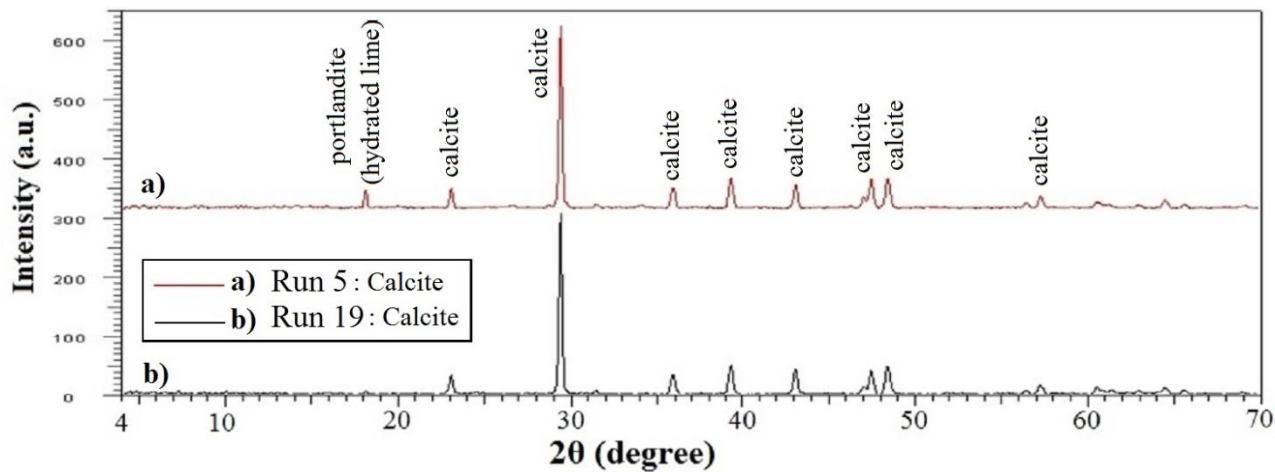
Figure S4. XRD Diffraction patterns of the crystal structure of the precipitated calcium carbonates. The X-ray diffraction patterns were done on a diffractometer (Bruker AXS, D8-Advance model) operated at 40 kV accelerating voltage and 30 A current, using Cu K_α radiation wavelength of 1.5418 Ă. The measurements were made at room temperature at a range of 4 to 70° on 2θ with a step size of 0.02°.
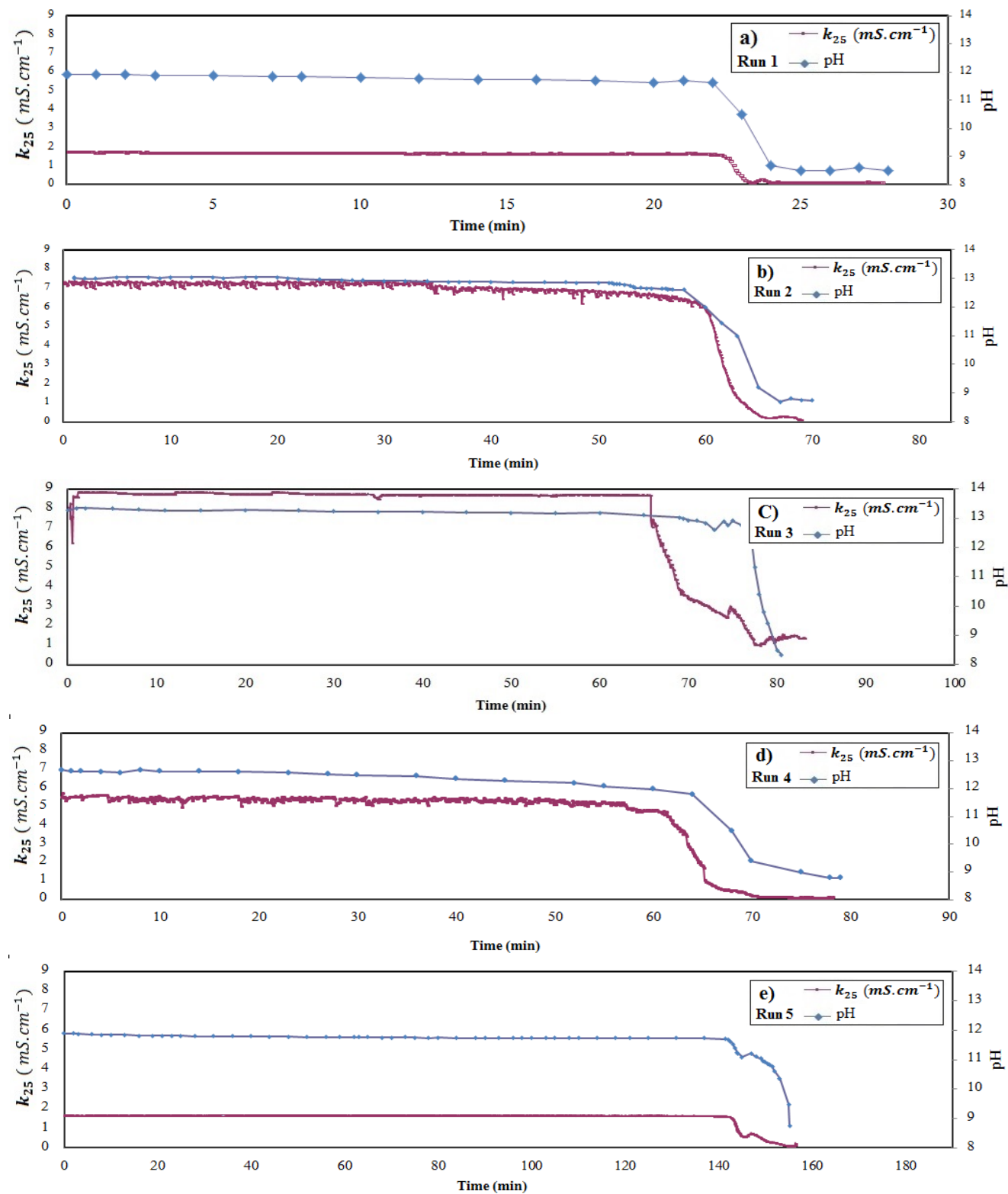
Supporting information S5:

Figure S5. FTIR spectra of CaCO$_3$ particles. The sharp absorption bands at 713 (v_4) and 874 cm^{-1} (v_2) suggest the presence of a calcite phase.
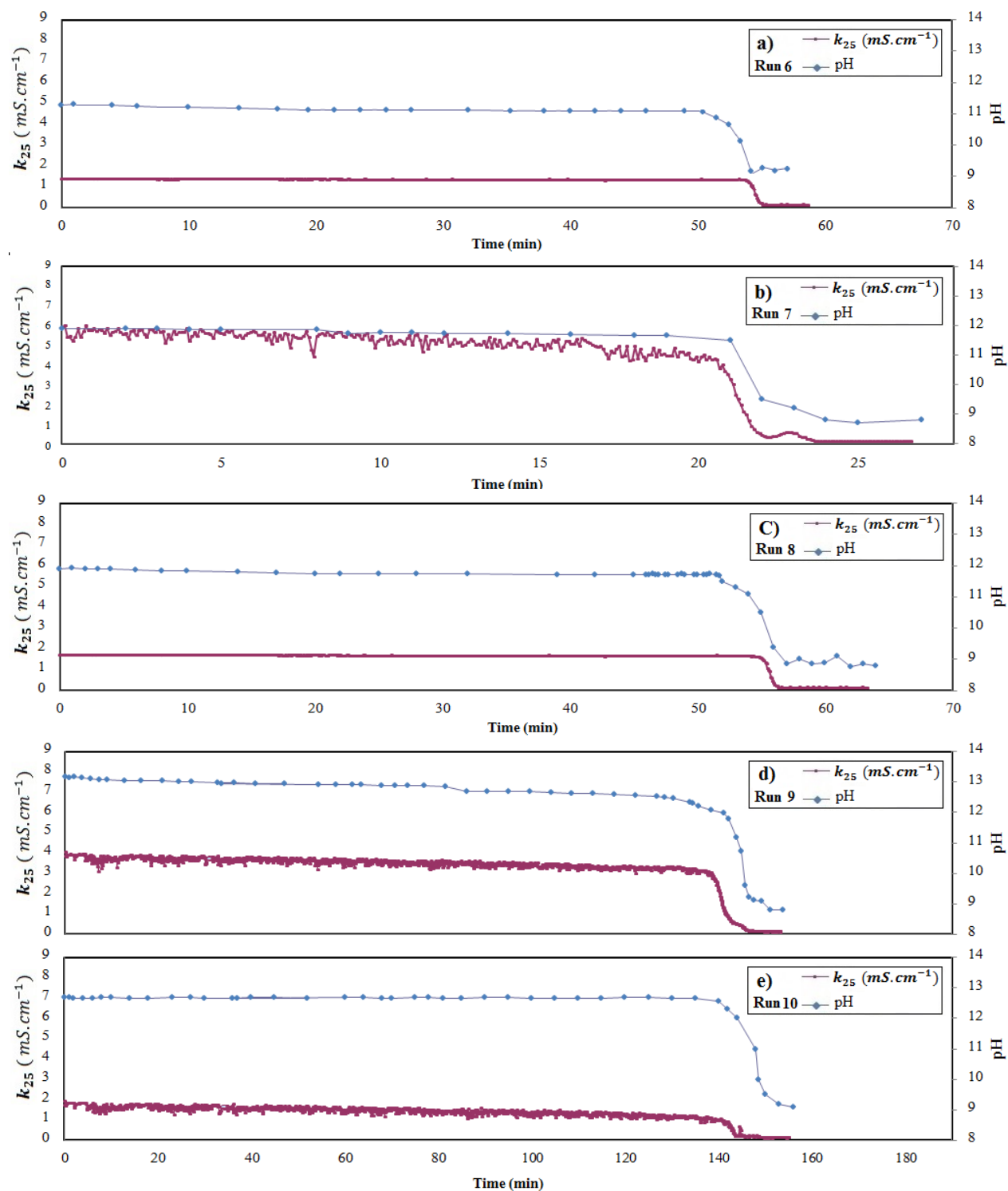
Supporting information S6:

Figure S6. The distribution logarithmic diagram as a function of pH for limited erea of the carbonation process. (c) for crystalline solids.

Supporting information S7:

Figure S7. Conductivity and pH variations during the carbonation tests along. **a**) Run 1, **b**) Run 2, **c**) Run 3, **d**) Run 4, **e**) Run 5.
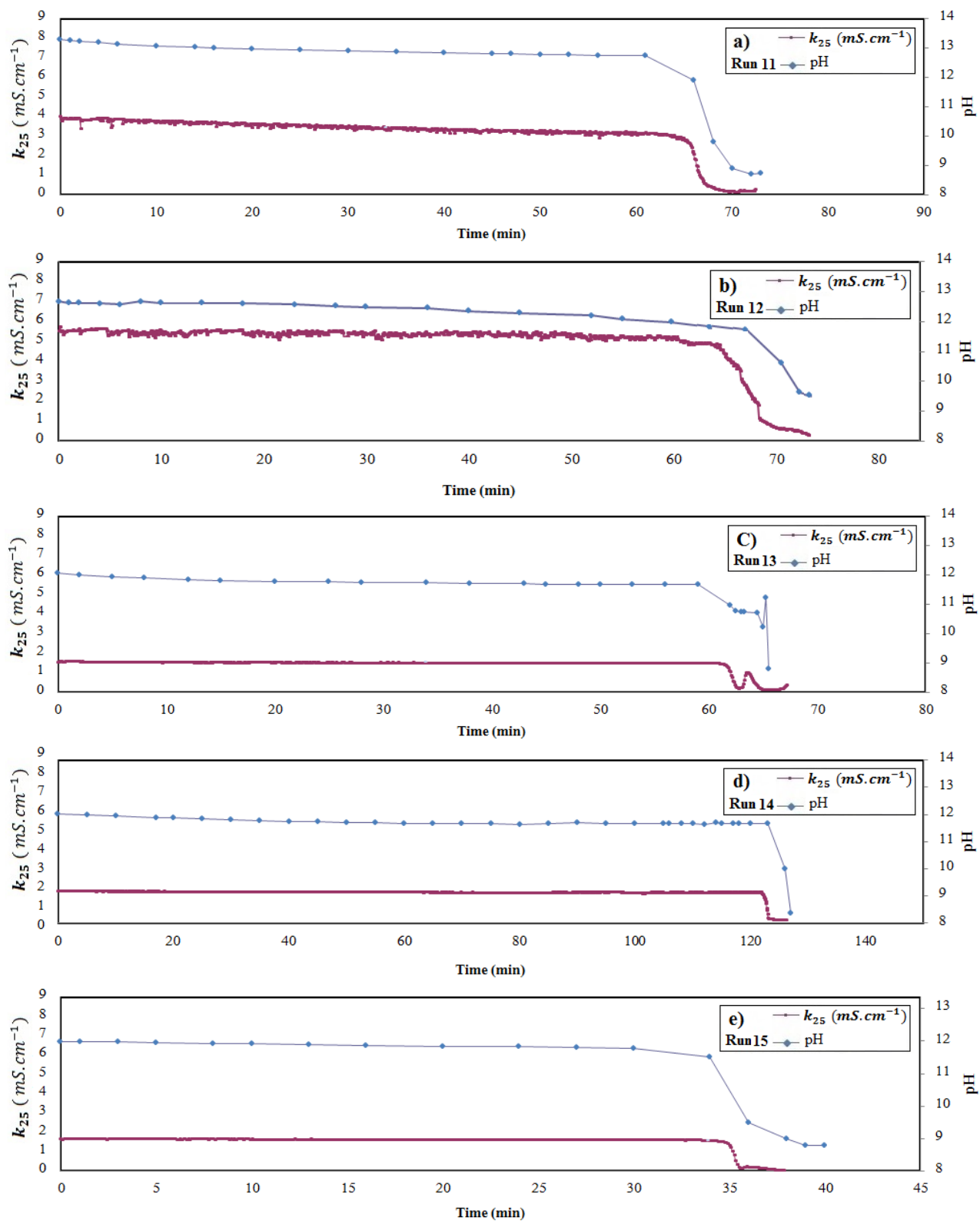
Supporting information S8:

Figure S8. Conductivity and pH variations during the carbonation tests along. **a**) Run 6, **b**) Run 7, **c**) Run 8, **d**) Run 9, **e**) Run 10.
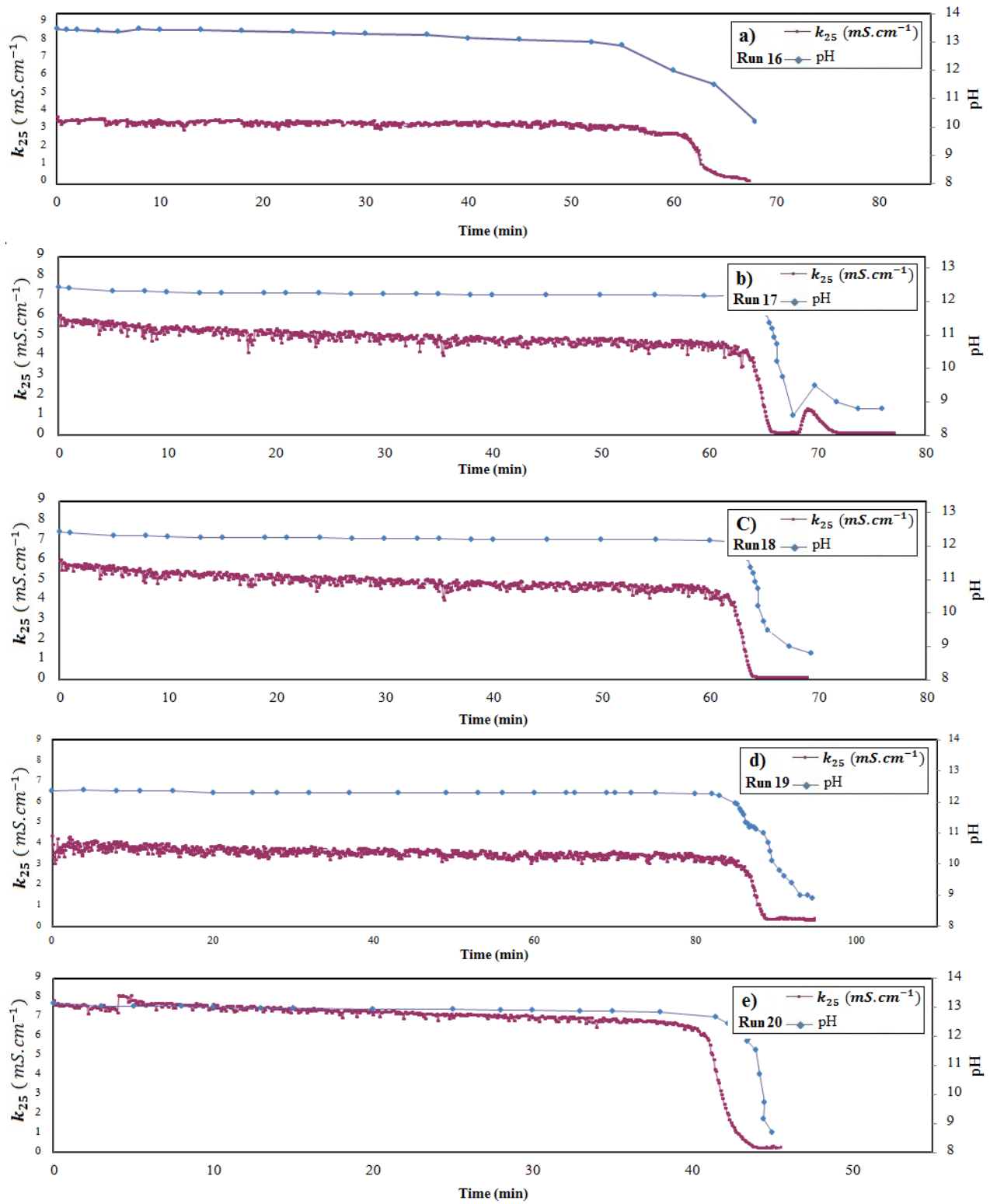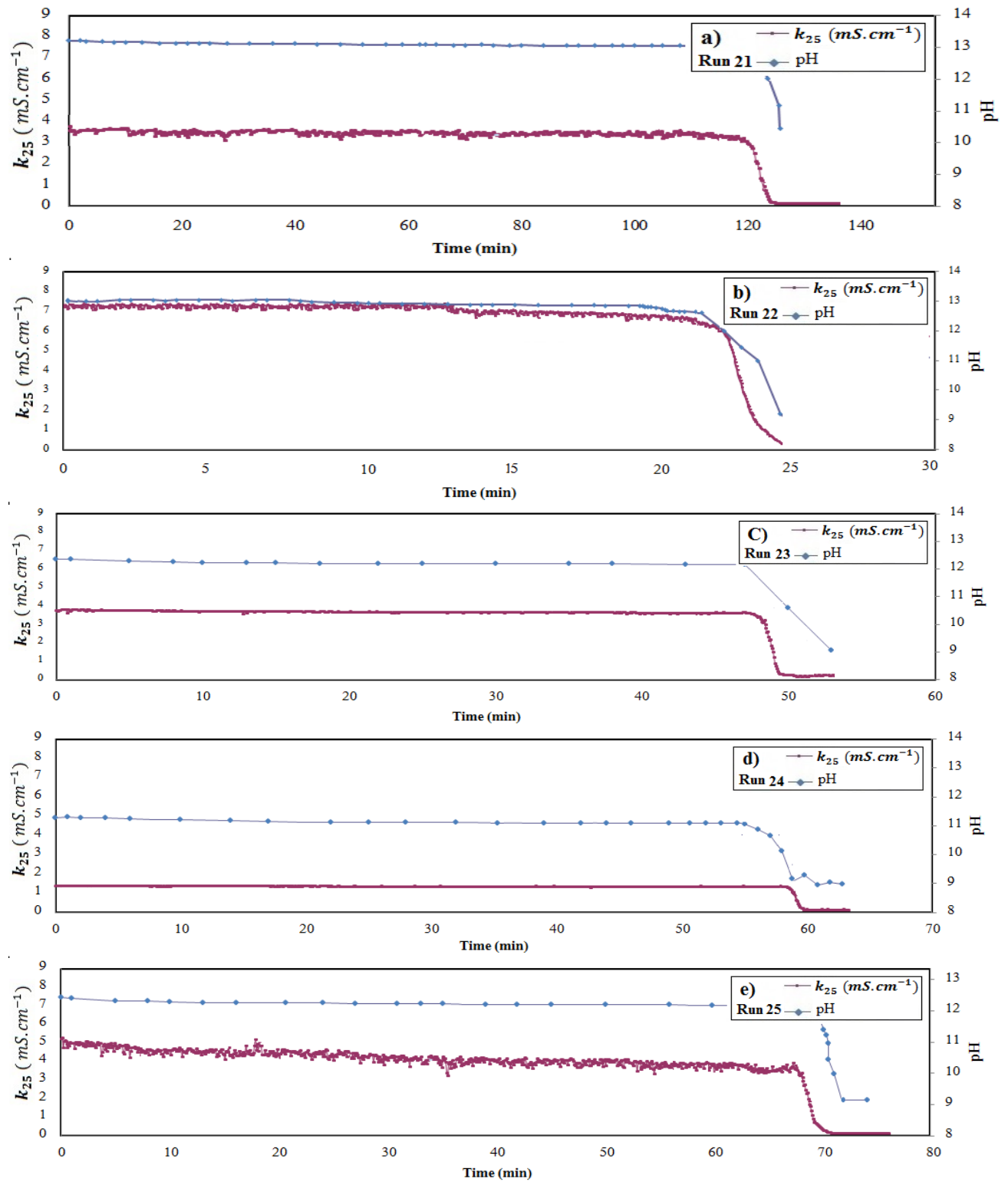
Supporting information S9:

Figure S9. Conductivity and pH variations during the carbonation tests along. **a)** Run 11, **b)** Run 12, **c)** Run 13, **d)** Run 14, **e)** Run 15.
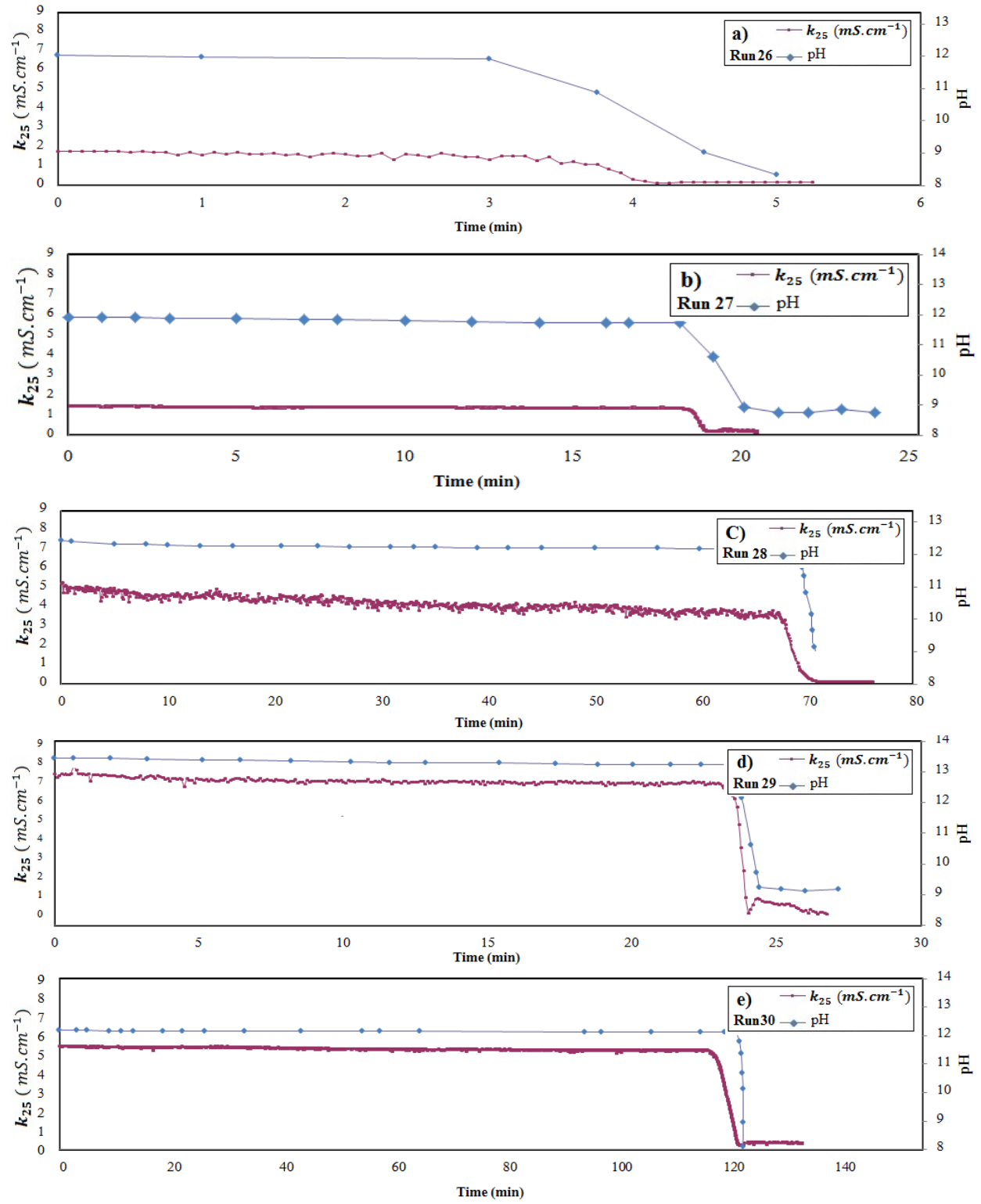
Supporting information S10:

Figure S10. Conductivity and pH variations during the carbonation tests along. **a**) Run 16, **b**) Run 17, **c**) Run 18, **d**) Run 19, **e**) Run 20.
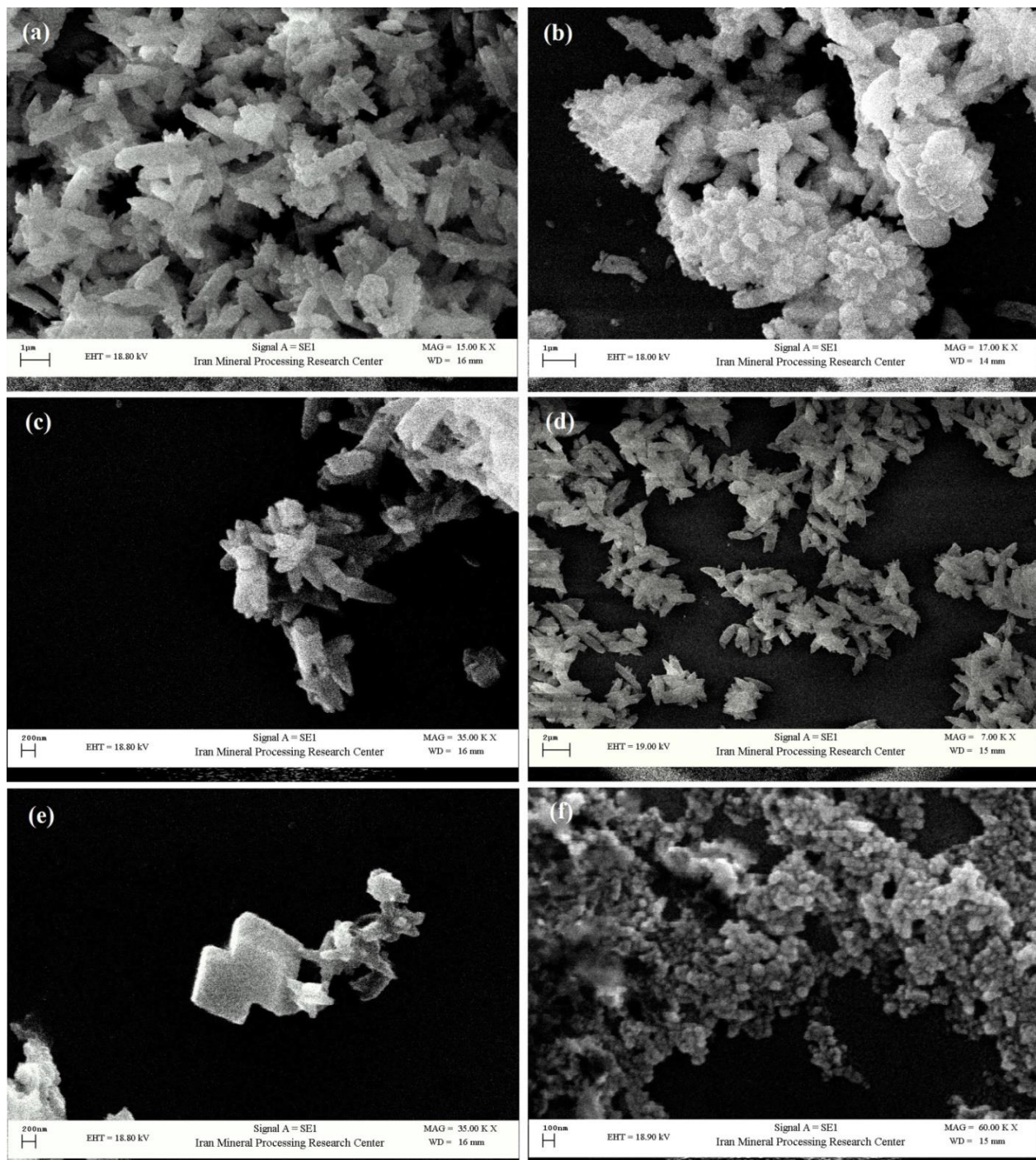
Supporting information S11:

Figure S11. Conductivity and pH variations during the carbonation tests along. **a**) Run 21, **b**) Run 22, **c**) Run 23, **d**) Run 24, **e**) Run 25.

Supporting information S12:

Figure S12. Conductivity and pH variations during the carbonation tests along. **a**) Run 26, **b**) Run 27, **c**) Run 28, **d**) Run 29, **e**) Run 30.

Supporting information S13:

Figure S13. SEM micrographs of various PCC morphologies in carbonation process. The specimens were coated by sputtering with gold (coating thickness approximately 320 nm) and examined under the Qemscan[TM], LEO 1450 VP scanning electron: a) elongated scalenohedral crystals, b) rosette-shape crystals growth, c) cluster scalenohedral crystals, d) scalenohedral crystals, e) rhombohedral crystals, and f) chain-like agglomerated nanoparticles
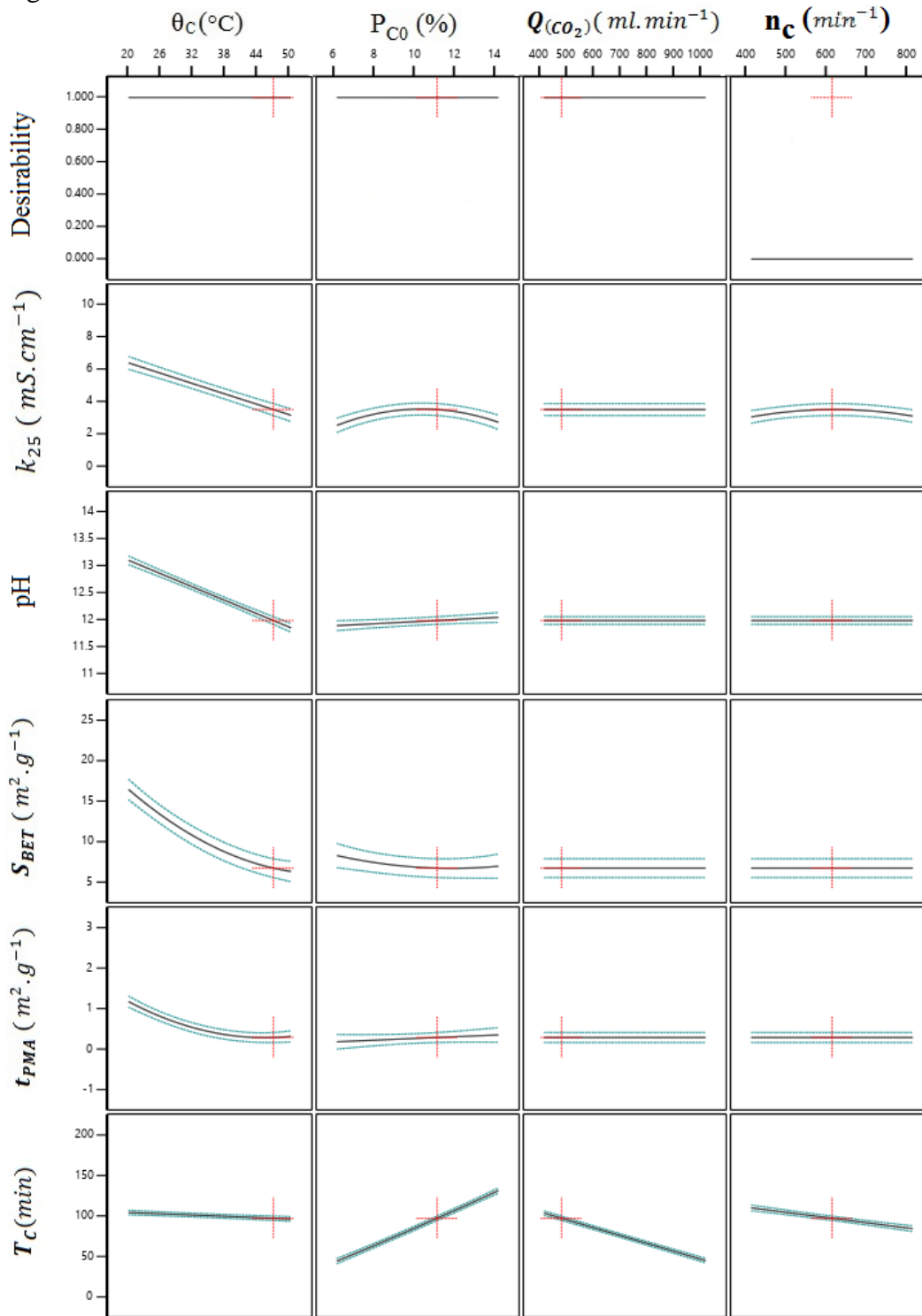
Figure S14. effect of temperature (θ_C), initial solid percent of the MOL suspension (P_{C0}), CO_2 gas flow rate $(Q(CO_2))$, and agitation rate (n_C) on the physical and chemical properties of PCC, including conductivity (κ_{25}), specific surface area (S_{BET}), microporous surface area (t_{PMA}) and subsequently agglomeration, reaction termination time (T_C), pH, and desirability values of parameters.
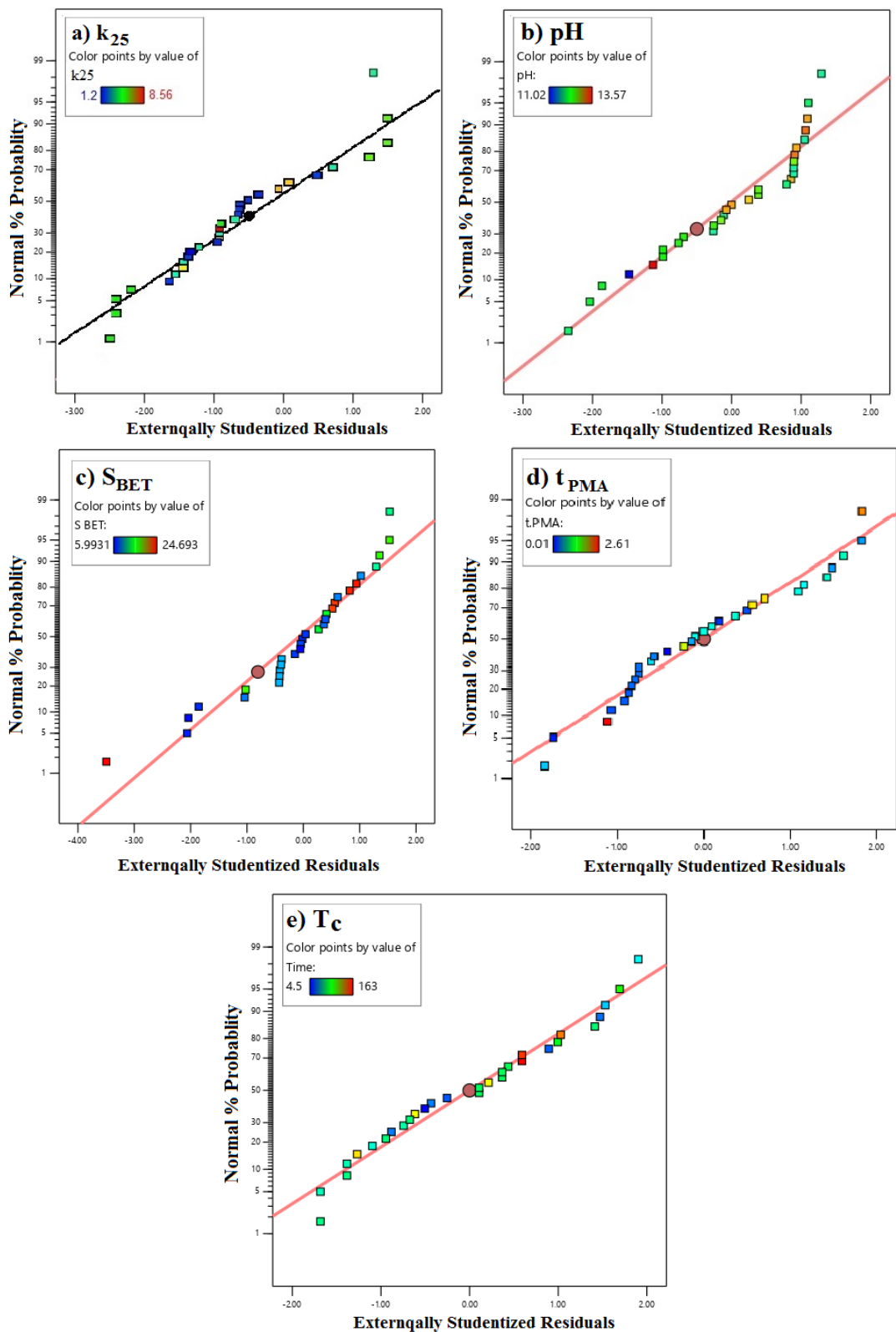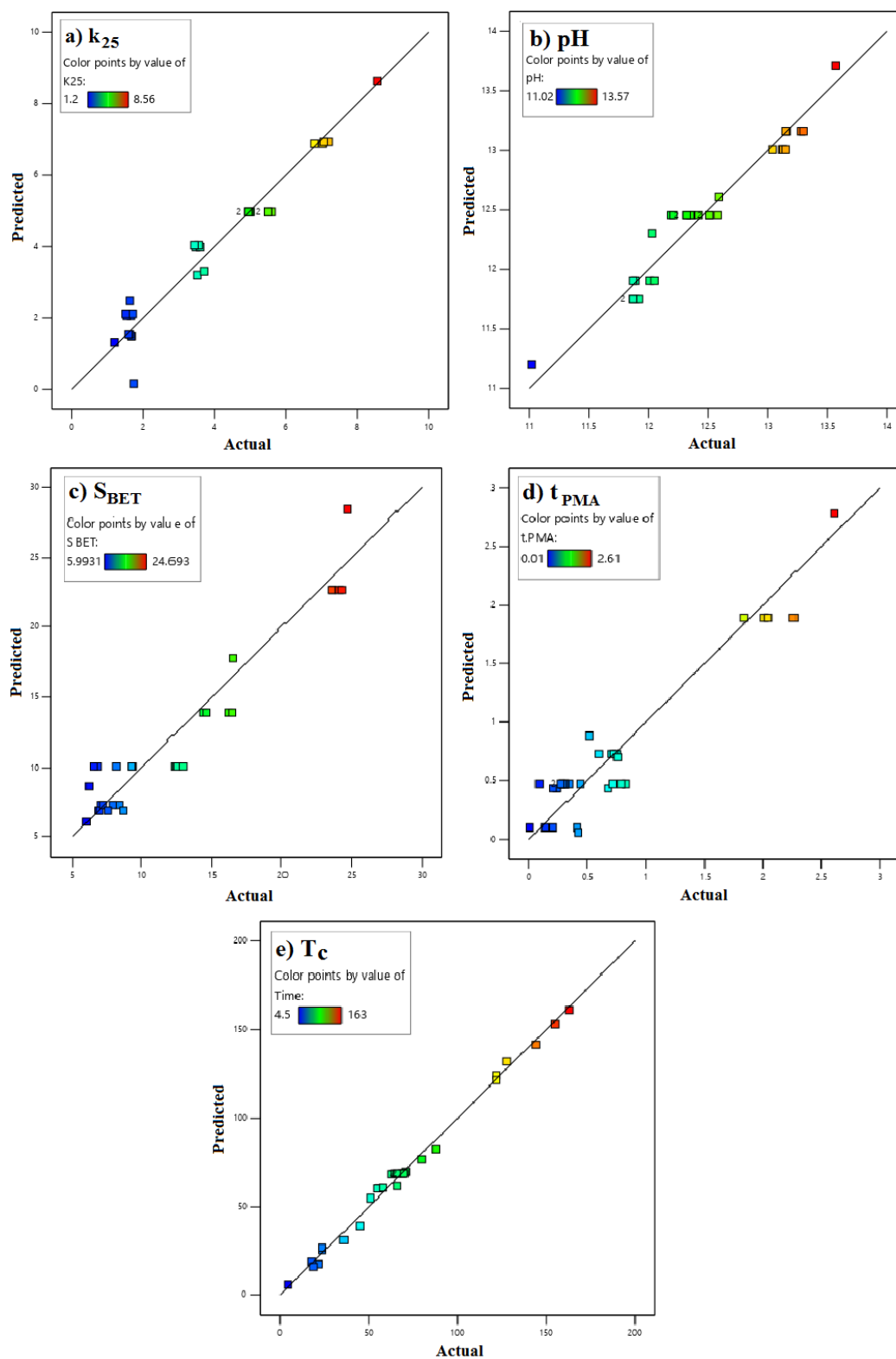
Supporting information S15:

Figure S15. Normal probability plots of residual for, a) κ_{25}, b) pH, c) S_{BET}, d) t_{PMA} , e) T_C

Supporting information S16:

Figure S16. Parity plots showing the distribution of experimental versus predicted data for response variables, a) κ_{25}, b) pH, c) S_{BET}, d) t_{PMA} , e) T_C
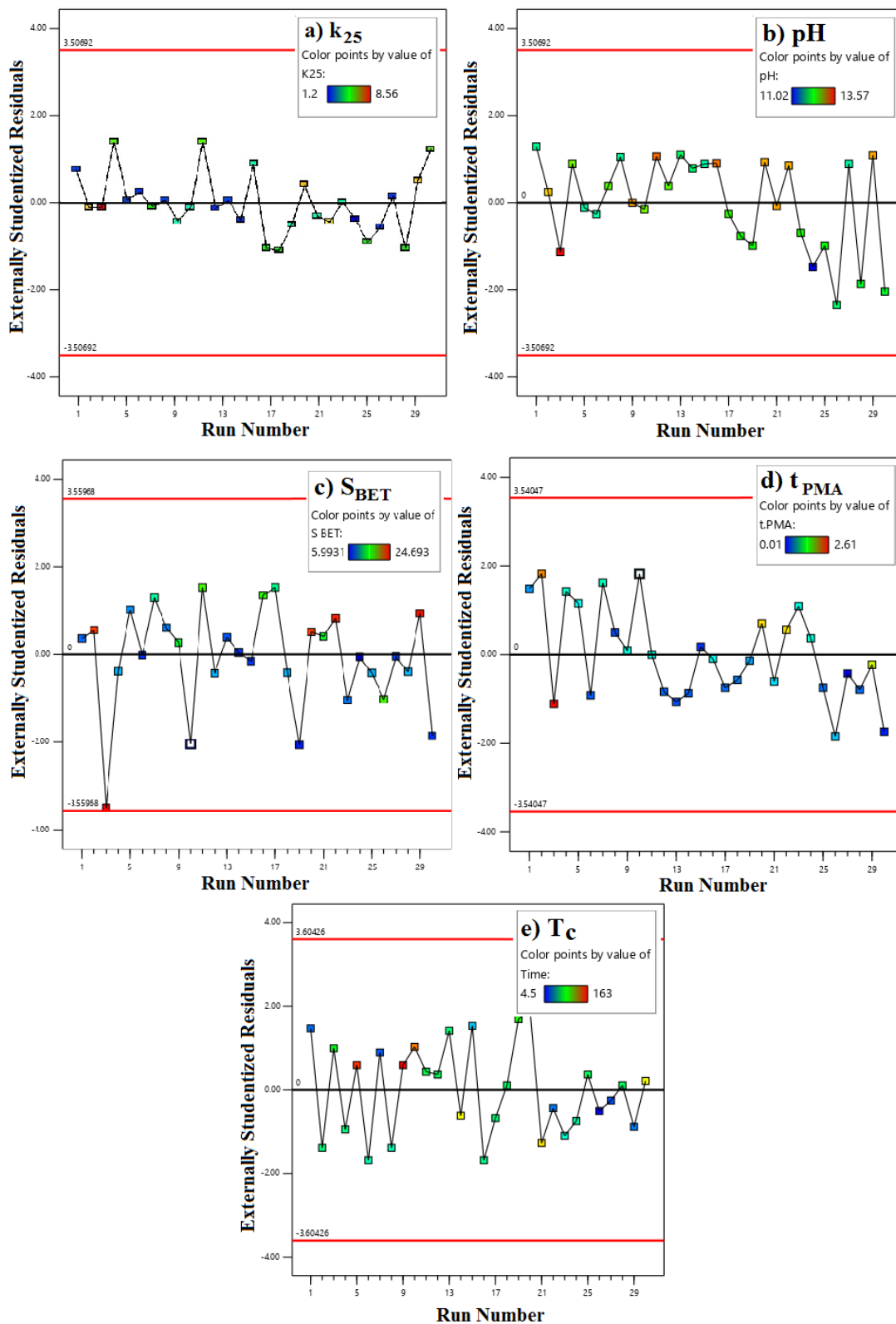
Supporting information S17:

Figure S17. Plot of residuals versus fitted values for, a) κ_{25}, b) pH, c) S_{BET}, d) t_{PMA} , e) T_C
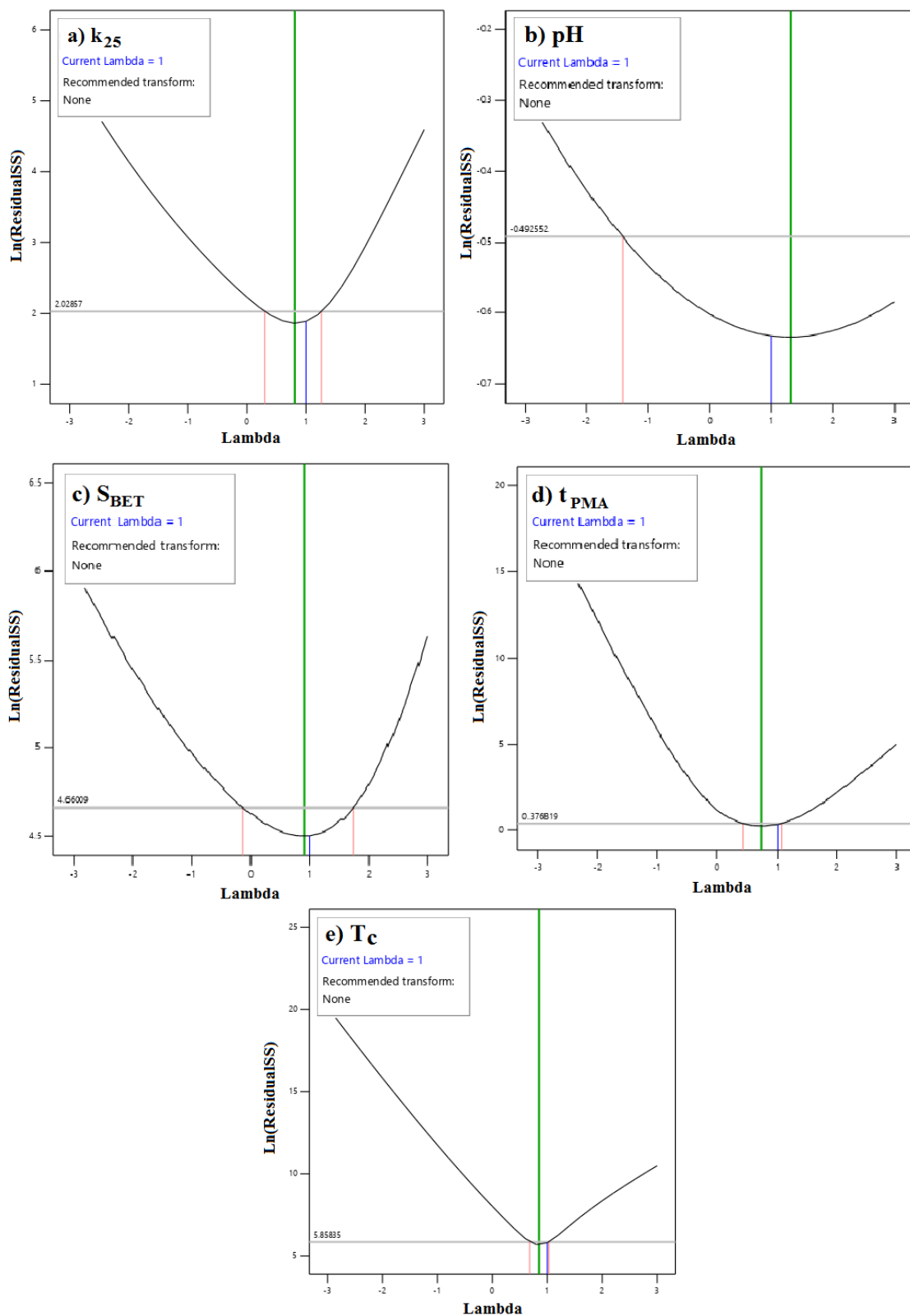
Supporting information S18:

Figure S18. Box-Cox Plot for Power Transforms, a) κ_{25}, b) pH, c) S_{BET}, d) t_{PMA} , e) T_C